study. *Environ Int* 2011; 37: 198–203.

38. **Takasuga T, Senthilkumar K, Takemori H, Ohi E, Tsuji H, Nagayama J.** Impact of fermented brown rice with *Aspergillus oryzae* (FEBRA) intake and concentrations of polybrominated diphenyl ethers (PBDEs) in blood of humans from Japan. *Chemosphere* 2004; 57: 795–811.

39. **Baker SE, Olsson AO, Barr OD.** Isotope dilution high-performance liquid chromatography–tandem mass spectrometry method for quantifying urinary metabolites of synthetic pyrethroid insecticides. *Arch Environ Contam Toxicol* 2004; 46: 281–288.

40. **Olsson AO, Baker SE, Nguyen JV, Romanoff LC, Udunka SO, Walker RD, Flemmen KL, Barr DB.** A liquid chromatography–tandem mass spectrometry multiresidue method for quantification of specific metabolites of organophosphorus pesticides, synthetic pyrethroids, selected herbicides, and deet in human urine. *Anal Chem* 2004; 76: 2453–2461.

41. **Kakimoto K, Akutsu K, Konishi Y, Tanaka Y.** Time trend of hexabromocyclododecane in the breast milk of Japanese women. *Chemosphere* 2007; 71: 1110–1114.

42. **Ueyama J, Saito I, Kamijima M, Nakajima T, Gotoh M, Suzuki T, Shibata E, Kondo T, Takagi K, Miyamoto K, Takamatsu J, Hasegawa T, Takagi K.** Simultaneous determination of urinary dialkylphosphate metabolites of organophosphorus pesticides using gas chromatography–mass spectrometry. *J Chromatogr B Analyt Technol Biomed Life Sci* 2006; 832: 58–66.

43. **Razagui IB, Ghribi I.** Maternal and neonatal scalp hair concentrations of zinc, copper, cadmium, and lead: relationship to some lifestyle factors. *Biol Trace Elem Res* 2005; 106: 1–28.

44. **Kondo F, Ikai Y, Goto T, Ito Y, Oka H, Nakazawa H, Odajima Y, Kamijima M, Shibata E, Torii S, Miyazaki Y.** Serum levels of volatile organic compounds in patients with sick building syndrome. *Bull Environ Contam Toxicol* 2006; 77: 331–337.

45. **Lehnertz B, Ueda Y, Derijck AA, Braunschweig U, Perez-Burgos L, Kubicek S, Chen T, Li E, Jenuwein T.** Peters, A.H., Suv39h-mediated histone H3 lysine 9 methylation

directs DNA methylation to major satellite repeats at pericentric heterochromatin. *Curr Biol* 2003; 13: 1192–1200.

46. **Senda S, Blanche S, Costagliola D, Cibert C, Nigon F, Firtion G, Floch C, Parat S, Viegas-Péquignot E.** Altered heterochromatin organization after perinatal exposure to zidovudine. *Antivir Ther* 2007; 12: 179–187.

47. **Xiong Z, Laird PW.** COBRA: a sensitive and quantitative DNA methylation assay. *Nucleic Acids Res* 1997; 25: 2532–2534.

48. **Eskenazi B, Marks AR, Bradman A, Harley K, Barr DB, Johnson C, Morga N, Jewell NP.** Organophosphate pesticide exposure and neurodevelopment in young Mexican–American children. *Environ Health Perspect* 2007; 115: 792–798.

49. **Harari R, Julvez J, Murata K, Barr D, Bellinger DC, Debes F, Grandjean P.** Neurobehavioral deficits and increased blood pressure in school-age children prenatally exposed to pesticides. *Environ Health Perspect* 2010; 118: 890–896.

50. **O'Shea KS.** Embryonic stem cell models of development. *Anat Rec* 1999; 257: 32–41.

51. **Kim H, Kang K, Kim J.** AEBP2 as a potential targeting protein for Polycomb Repression Complex PRC2. *Nucleic Acids Res* 2009; 37: 2940–2950.

52. **Heng JI, Nguyen L, Castro DS, Zimmer C, Wildner H, Armant O, Skowronska-Krawczyk D, Bedogni F, Matter JM, Hevner R, Guillemot F.** Neurogenin 2 controls cortical neuron migration through regulation of Rnd2. *Nature* 2008; 455: 114–118.

53. **Okuda H, Miyata S, Mori Y, Tohyama M.** Mouse Prickle1 and Prickle2 are expressed in postmitotic neurons and promote neurite outgrowth. *FEBS Lett* 2007; 581: 4754–4760.

54. **Benke GM, Murphy SD.** The influence of age on the toxicity and metabolism of methyl parathion and parathion in male and female rats. *Toxicol Appl Pharmacol* 1975; 31: 254–269.

55. **Chakraborti TK, Farrar JD, Pope CN.** Comparative neurochemical and neurobehavioral effects of repeated chlorpyrifos exposures in young and adult rats. *Pharmacol Biochem Behav* 1993; 46: 219–224.

56. **Jiang G, Xu L, Song S, Zhu C, Wu Q, Zhang L, Wu L.** Effects of long-term low-dose cadmium exposure on genomic DNA methylation in human embryo lung fibroblast cells. *Toxicology* 2008; 244: 49–55.

57. **Xiang N, Zhao R, Song G, Zhong W.** Selenite reactivates silenced genes by modifying DNA methylation and histones in prostate cancer cells. *Carcinogenesis* 2008; 29: 2175–2181.

58. **Ramachandran K, Navarro L, Gordian E, Das PM, Singal R.** Methylation-mediated silencing of genes is not altered by selenium treatment of prostate cancer cells. *Anticancer Res* 2007; 27: 921–926.

FIGURE LEGENDS

Figure 1. Outline of the chemical exposure experiments. The scheme of culture conditions for mouse ESCs or EBs is illustrated as Exp. 1–4. ESCs were cultured under stem cell conditions (+LIF) with one of the 25 chemicals that have been detected in the serum of pregnant mothers or fetal cord blood (Table 1), at serum level or tenfold higher than serum level concentrations. After 48-hr exposure of cells to the individual chemicals, the heterochromatin status in the nuclei was analyzed to assess whether the chemicals have potential as epimutagens (Exp. 1). Next, to test whether chemical exposure causes alteration in DNA methylation at unique gene loci (Exp. 2) and whether chemical-induced heterochromatin changes are reversible or not (Exp. 3), we cultured ESCs with five chemicals that were determined as epimutagens in Exp. 1. Finally, cells were exposed to chemicals at serum level during EB formation to investigate whether the chemicals affect cellular differentiation (Exp. 4)

Figure 2. Establishment of an epimutagen screening method and identification of epimutagen candidates by heterochromatin staining in mouse ESCs.

(*A*) Visualization of heterochromatin structure in nuclei by DAPI staining, immunofluorescence, and DNA-FISH. Signal intensities of DAPI, HP1a, or major satellite on the dotted lines (a–b or c–d) were measured and plotted. The strong DAPI signals (filled triangles) were confirmed to merge with the two heterochromatin markers, HP1a, and major satellite signals.

(*B*) Confirmation of altered heterochromatin by DAPI staining of mouse ESCs with a known epimutagen, TSA. After 48-hr exposure of ESCs to TSA (0, 0.2, or 1.0 nM), the cells were stained with DAPI, and the number of DAPI dense signals per interphase nucleus was determined with ImageJ software. The number of signals is shown as a box plot. Statistical comparisons of signal numbers were performed using the Wilcoxon test. *, $p < 0.01$.

(*C*) Effect of solvent on number of DAPI signals. The numbers of DAPI signals were counted and plotted as in (*B*). –, without solvent

(*D*) Number of DAPI signals in nuclei of ESCs exposed to chemicals. ESCs were cultured with chemicals that were categorized into seven groups (A–G) for 48 hr at serum level or tenfold higher

level than serum concentrations. The number of DAPI signals in the nuclei was determined with ImageJ software. Statistical comparisons of signal numbers were performed by the Wilcoxon test. *, $p < 0.01$. ND, Not determined; cells died of chemical exposure.

(*E*) Confirmation of heterochromatin changes in nuclei of mouse ESCs, exposed to DEP, Hg, cotinine, Se, or S-421 by major satellite staining. Heterochromatin in interphase nuclei was visualized by DNA-FISH with a specific probe for a heterochromatin marker, major satellite (red), and by DAPI staining (blue). Scale bar = 10 μm.

(*F*) Size of heterochromatin signals in nuclei of chemical-exposed ESCs. In the graph, the longitudinal and horizontal axes represent the average size and number of major satellite signals in nuclei by DNA-FISH analysis, respectively.

Figure 3. Effect of chemicals on DNA methylation in ESCs.

(*A*) Analysis of DNA methylation status in chemical-exposed ESCs by COBRA assay. ESCs were cultured with chemicals (DEP, Hg, cotinine, Se, and S-421) at the serum level concentrations or their solvents for 96 hr. Inset indicates the workflow of COBRA. DNA methylation degree (%) was calculated by the ratio of digested (methylated) and undigested (unmethylated) fragments. In the graph, each plot shows the methylation level of the individual gene locus that was examined. The longitudinal and horizontal axes represent the methylation level of chemical- and solvent-exposed samples, respectively. Plots that are located near the diagonal line mean similar methylation levels between chemical-exposed and solvent-treated cells. In the case of plots that are away from the diagonal line, methylation levels are different between the two samples. Open and closed plots located inside or outside the dotted line show that the difference in the methylation level between chemical- and solvent-exposed cells was within or over 5%, respectively.

(*B*) Methylation status at the *Rnd2*, *Aebp2*, and *Prickle2* T-DMRs by COBRA assay. DNA methylation degree (%) is shown as the average ± SE. *Rnd2* became more methylated upon Hg exposure, and *Aebp2* and *Prickle2* exhibited reduced methylation degrees after Se exposure. The positions of the *Hpy* CH4 IV site are illustrated as triangles. Black boxes represent exons, and the first

exon is only represented in the *Aebp2* and *Prickle2* genes. Statistical comparisons of DNA methylation were performed using the Student's *t* test. *, $p < 0.01$.

Figure 4. Reversibility of heterochromatin alteration and developmental effect of the five chemicals.

(*A*) Effect of chemicals on heterochromatin states after removal of chemicals. ESCs were cultured with either of the chemicals (DEP, Hg, cotinine, Se, and S-421) at the serum level-concentrations or solvent only for 48 hr, and then continued to culture without chemicals or solvent (control) for another 48 hr. The results are shown as a box plot. DNA-FISH analysis with a specific DNA probe for major satellite repeats in ESCs after removal of DEP. Localizations of major satellite repeats (red), DAPI-stained DNA (blue), and the merged images are shown. Scale bar = 10 μm. Statistical comparisons of DAPI signal number were performed using the Wilcoxon test. *, $p < 0.01$.

(*B*) Impaired EB formation by chemical exposure at the serum level concentrations. ESCs induced differentiation into EBs in the presence of one of the five chemicals (DEP, Hg, cotinine, Se, and S-421). Size of EBs exposed to chemicals at the serum level concentrations was measured as their areas by ImageJ. Average and SE of areas in EBs were calculated. Relative areas in chemical-exposed EBs were normalized to average areas of solvent-exposed control EBs. Experiments were performed at least twice independently for each chemical. −, solvent only; +, exposure to chemicals at the serum level concentrations. Scale bar = 250 μm. Statistical comparisons of area of EBs were performed using the Student's *t* test. *, $p < 0.01$.

(*C*) Summary of heterochromatin analysis based on the DAPI staining (Exp. 1, 3 in Fig. 1) and EB formation (Exp. 4 in Fig. 1). ↑, increase; ↓, decrease; →, no change of DAPI signal number or size of EBs compared with solvent-treated controls; ND, not determined.

Exp.1 Epimutagen screening
(25 chemicals detected in human samples)

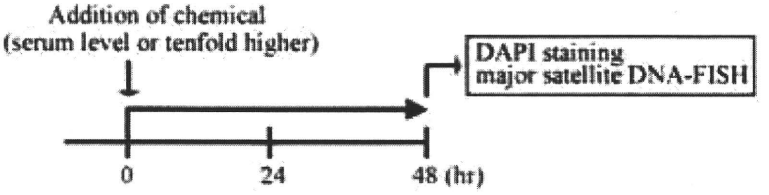

Exp.2 DNA methylation analysis
(DEP, Hg, cotinine, Se or S-421 exposed cells)

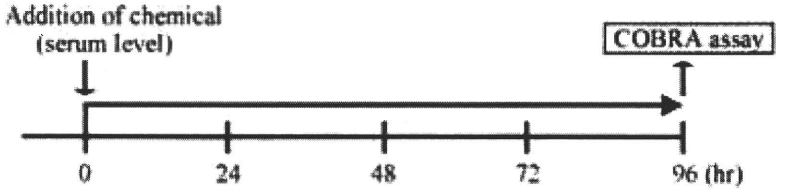

Exp.3 Reversibility of heterochromatin changes
(epimutagen candidate DEP, Hg, cotinine, Se, S-421)

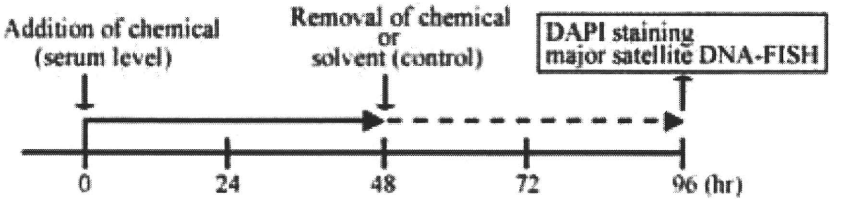

Exp.4 EB formation
(DEP, Hg, cotinine, Se or S-421 exposed cells)

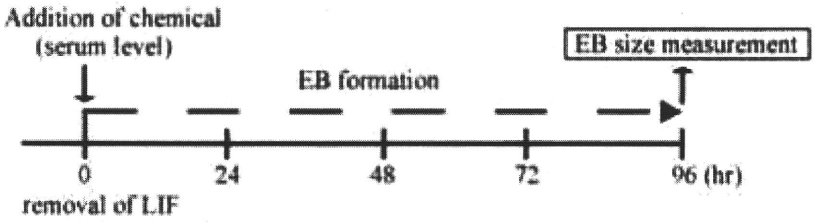

Fig. 1

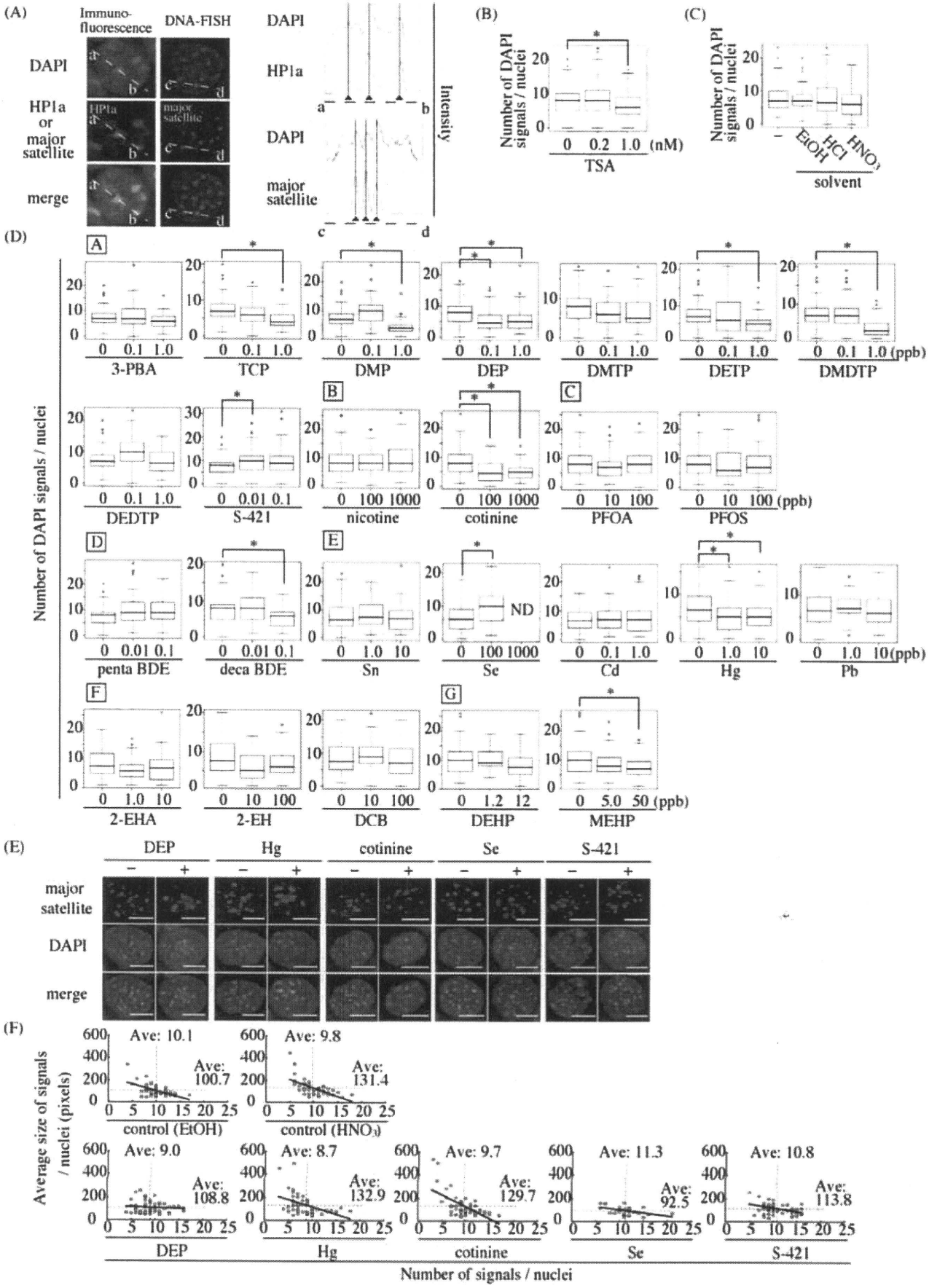
(A)
Immuno-fluorescence
DNA-FISH
DAPI
HP1a or major satellite
merge
DAPI
HP1a
major satellite
Intensity
(B)
Number of DAPI signals / nuclei
TSA
0 0.2 1.0 (nM)
(C)
Number of DAPI signals / nuclei
EtOH
HCl
HNO3
solvent
(D)
Number of DAPI signals / nuclei
3-PBA
TCP
DMP
DEP
DMTP
DETP
DMDTP
DEDTP
S-421
nicotine
cotinine
PFOA
PFOS
penta BDE
deca BDE
Sn
Se
Cd
Hg
Pb
2-EHA
2-EH
DCB
DEHP
MEHP
ND
(ppb)
(E)
DEP
Hg
cotinine
Se
S-421
major satellite
DAPI
merge
(F)
Average size of signals / nuclei (pixels)
Number of signals / nuclei
control (EtOH)
control (HNO3)
DEP
Hg
cotinine
Se
S-421

Fig. 2

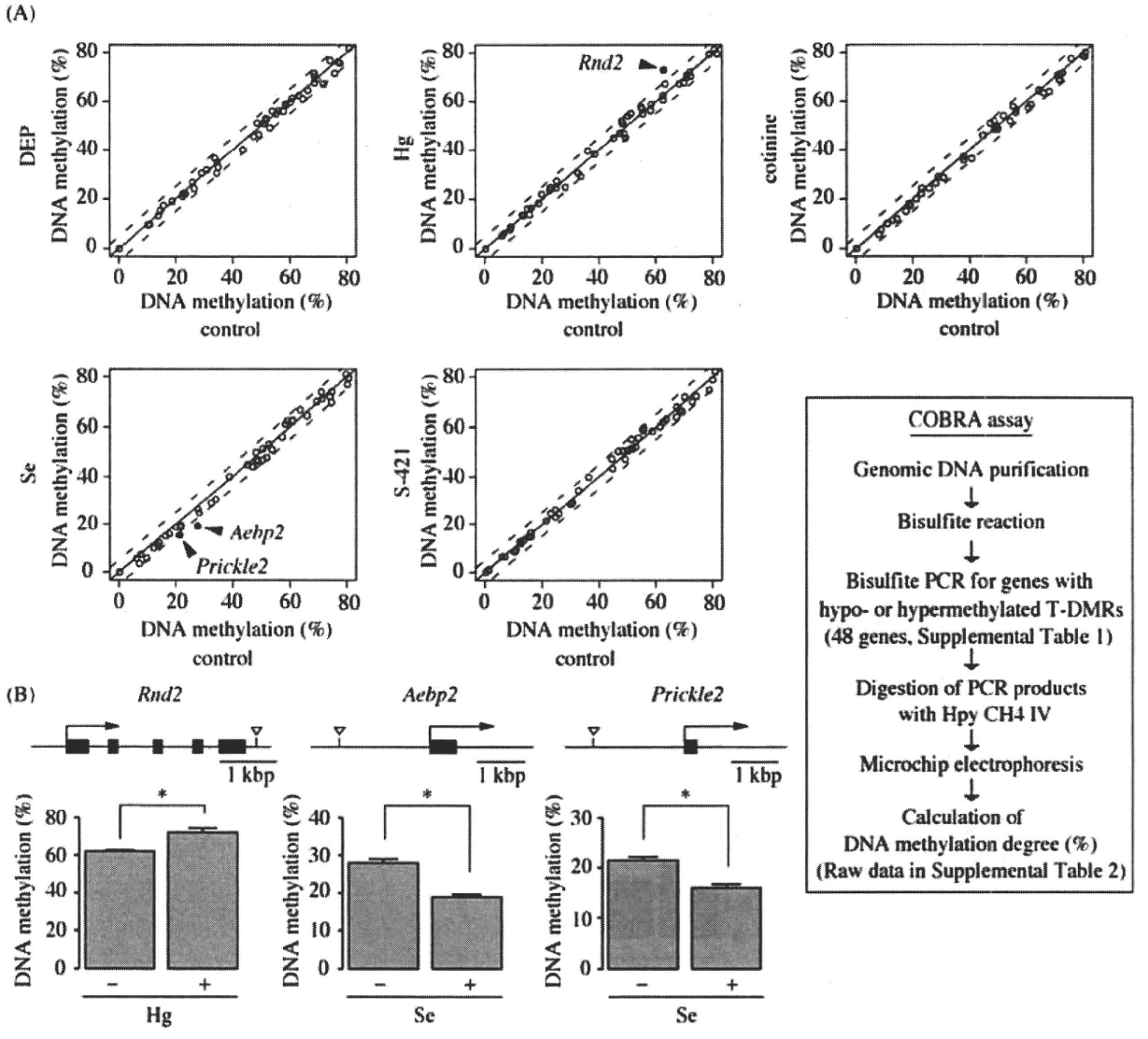
(A)
DEP
Hg
cotinine
Se
S-421
DNA methylation (%)
control
Rnd2
Aebp2
Prickle2
COBRA assay
Genomic DNA purification
Bisulfite reaction
Bisulfite PCR for genes with hypo- or hypermethylated T-DMRs (48 genes, Supplemental Table 1)
Digestion of PCR products with Hpy CH4 IV
Microchip electrophoresis
Calculation of DNA methylation degree (%) (Raw data in Supplemental Table 2)
(B)
Rnd2
Aebp2
Prickle2
1 kbp
DNA methylation (%)
Hg
Se
Se

Fig. 3

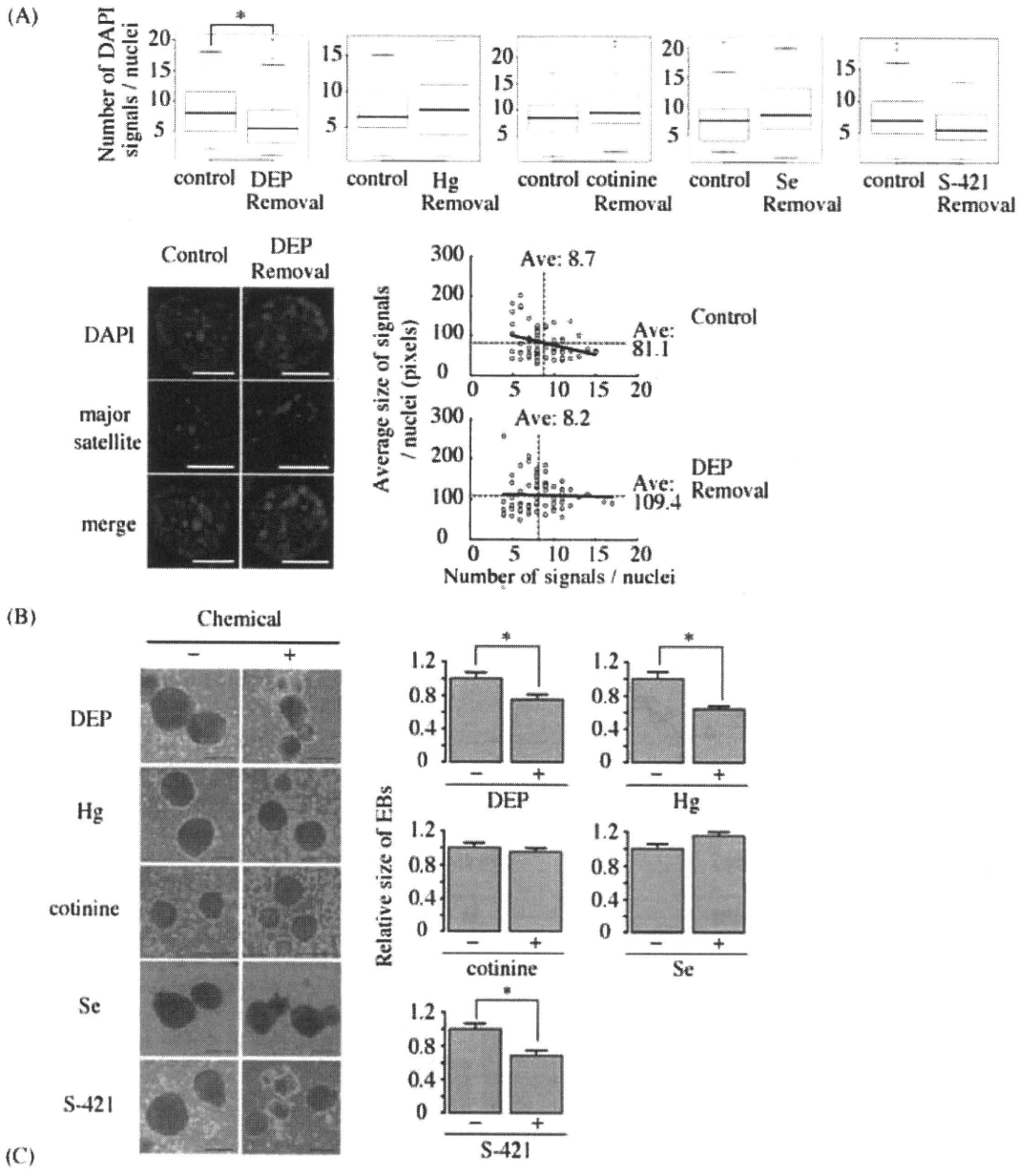

	chemical	exposure to cells (ppb) (×1, ×10)	DAPI signals (Exp.1) chemical exposure ×1, ×10	DAPI signals (Exp.3) Removal of chemicals	(Exp.4) Size of EBs
A	3-PBA	0.1, 1.0	→ →	ND	ND
	TCP	0.1, 1.0	→ ⇩	ND	ND
	DMP	0.1, 1.0	→ ⇩	ND	ND
	DEP	0.1, 1.0	⇩ ⇩	⇩	⇩
	DMTP	0.1, 1.0	→ →	ND	ND
	DETP	0.1, 1.0	→ ⇩	ND	ND
	DMDTP	0.1, 1.0	→ ⇩	ND	ND
	DEDTP	0.1, 1.0	→ →	ND	ND
	S-421	0.01, 0.1	⇧ →	→	⇩
B	nicotine	100, 1000	→ →	ND	ND
	cotinine	100, 1000	⇩ ⇩	→	→
C	PFOA	10, 100	→ →	ND	ND
	PFOS	10, 100	→ →	ND	ND

	chemical	exposure to cells (ppb) (×1, ×10)	DAPI signals (Exp.1) chemical exposure ×1, ×10	DAPI signals (Exp.3) Removal of chemicals	(Exp.4) Size of EBs
D	penta BDE	0.01, 0.1	→ →	ND	ND
	deca BDE	0.01, 0.1	→ ⇩	ND	ND
E	Sn	1.0, 10	→ →	ND	ND
	Se	100, 1000	⇧ ND	→	→
	Cd	0.1, 1.0	→ →	ND	ND
	Hg	1.0, 10	⇩ ⇩	→	⇩
	Pb	1.0, 10	→ →	ND	ND
F	2-EHA	1.0, 10	→ →	ND	ND
	2-EH	10, 100	→ →	ND	ND
	DCB	10, 100	→ →	ND	ND
G	DEHP	1.2, 12	→ →	ND	ND
	MEHP	5.0, 50	→ ⇩	ND	ND

Fig. 4

Research Article

Biomedical Chromatography

Received 15 April 2010, Revised 10 May 2010, Accepted 11 May 2010 Published online in Wiley Online Library: 16 July 2010

(wileyonlinelibrary.com) DOI 10.1002/bmc.1475

Development and validation of a hydrophilic interaction chromatography–tandem mass spectrometry for quantification of nicotine and its metabolites in human maternal and cord sera

Yusuke Iwasaki[a], Masato Goto[a], Keisuke Mochizuki[a], Emi Terayama[a], Rie Ito[a], Koichi Saito[a], Norihiro Sugino[b], Tsunehisa Makino[c] and Hiroyuki Nakazawa[a]*

ABSTRACT: A selective and sensitive HILIC-MS/MS method for the simultaneous quantification of nicotine and its metabolites in human maternal and cord sera was developed and validated. After solid-phase extraction, LC separation was achieved on a hydrophilic interaction chromatography. The validated method is capable of selective identification as well as accurate and sensitive quantification. Analyte recovery ranged from 86.2 to 107.7% and intra- and inter-day assay precision were less than 15% relative standard deviation. This sensitive HILIC-MS/MS method can be used to determine nicotine and its metabolic profile in smokers. This validated method is useful for the determination of nicotine and its metabolites in human serum in future studies of the effects of nicotine exposure on neonatal outcome. Copyright © 2010 John Wiley & Sons, Ltd.

Keywords: nicotine; metabolite; hydrophilic interaction chromatography; tandem mass spectrometry; serum

Introduction

Nicotine (NIC), the principal active constituent and primary alkaloid in tobacco products, is a widely consumed natural product. NIC is the major tobacco-specific component in both mainstream tobacco smoke and environmental tobacco smoke (ETS). NIC contributes to diseases that are related to smoking.

There are numerous reports on tobacco-related health risks in women, children and neonates. Women are at risk of lung cancer (Freedman *et al.*, 2008), hypertension (Bowman *et al.*, 2007), chronic obstructive pulmonary disease and cancer (Pope *et al.*, 1999). For the fetus, maternal smoking is associated with premature birth and intrauterine growth restriction (Andres and Day, 2000; Bouckaert, 2000). Neonates and young children who are exposed to second-hand smoke in their homes are at an increased risk of the development of asthma and other respiratory disorders later in childhood, and death from the sudden infant death syndrome (Windham *et al.*, 2000).

NIC reaches the central nervous system (CNS) within 20 s of tobacco smoke inhalation; it has a plasma half-life of 2–4 h and a brain half-life of 52 min (Benowitz *et al.*, 1994). Because of the health risks associated with tobacco exposure, research into suitable biomarkers of tobacco smoke exposure has surged (Pérez-Stable *et al.*, 1995; Benowitz, 1996). Smoking is one of the main causes of newborn premature death in Japan and has been shown to increase the incidence of various types of cancers (Seltzer, 2003). Smokers generally have plasma cotinine (COT) levels higher than 15 ng/mL, while heavy smokers (>20 cigarettes/day) usually have levels higher than 300 ng/mL. Second-hand smoke, or ETS, has been an area of active study in the health sciences for several decades. The National Health and Nutrition Examination Survey data from 1988 to 1991 showed that 88% of non-smokers in the USA had detectable concentrations of serum COT (Pirkle *et al.*, 1996), which is one of the major oxidative metabolites of NIC, accounting for 70–80% of NIC metabolites in serum (Hukkanen *et al.*, 2005). COT has a relatively long half-life of 10–40 h in humans (Russell and Feyerabend, 1978), which makes it a suitable marker to assess the exposure to tobacco smoke.

* Correspondence to: H. Nakazawa, Department of Analytical Chemistry, Faculty of Pharmaceutical Sciences, Hoshi University, 2-4-41 Ebara, Shinagawa-ku, Tokyo 142-8501, Japan. E-mail: nakazawa@hoshi.ac.jp

[a] Department of Analytical Chemistry, Faculty of Pharmaceutical Sciences, Hoshi University, Tokyo, Japan

[b] Department of Obstetrics and Gynecology, Yamaguchi University Graduate School of Medicine, Ube, Japan

[c] Toubu Hospital, Shizuoka, Japan

Abbreviation used: *COT, cotinine; ETS, environmental tobacco smoke;* HCOT, *trans*-3′-hydroxycotinine; NCOT, norcotinine; NIC, nicotine; NNIC, nornicotine.

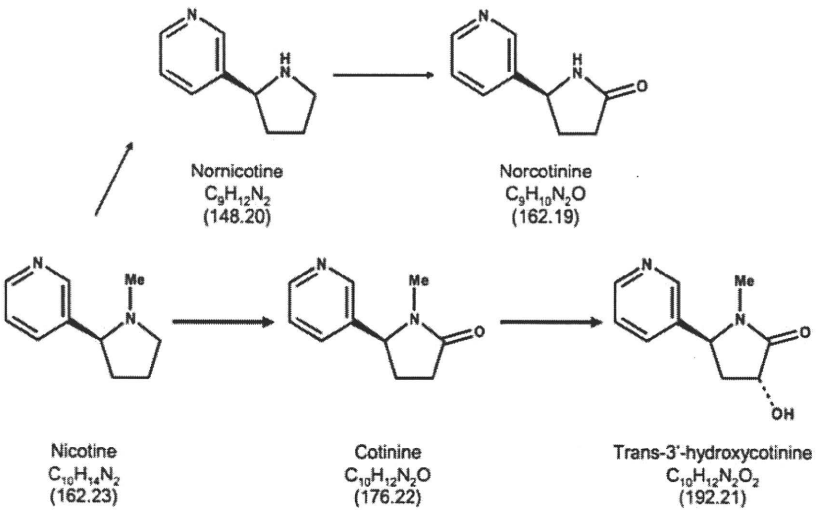

Figure 1. Chemical structures of nicotine and its metabolites.

Table 1. MRM conditions for the analysis of nicotine and its metabolites

Compound	Precursor ion (*m/z*)	Product ion (*m/z*)	Cone voltage (V)	Collision voltage (V)
NNIC	149.2	130.3	28	18
NIC	163.0	130.3	30	20
NCOT	163.2	80.0	38	23
COT	176.9	80.0	35	22
HCOT	193.2	79.9	39	23
NNIC-d_4	153.2	134.3	28	18
NIC-d_3	166.0	130.3	30	20
NCOT-d_4	167.2	84.0	38	23
COT-d_3	179.9	80.0	35	22
HCOT-d_3	196.2	79.9	39	23

When inhaled, tobacco smoke is efficiently absorbed from the lung, where 82–92% of NIC is absorbed into the pulmonary circulation, followed by rapid permeation through the blood–brain barrier (Lockman *et al.*, 2005).

A variety of methods have been reported for the determination and quantification of NIC and its metabolites in biological fluids, i.e. serum, urine, saliva and whole blood. These include high-performance liquid chromatography (HPLC) (Pacifici *et al.*, 1993; Abu-Qare and Abou-Donia, 2001) and gas chromatography–mass spectrometry (GC-MS) (Davoli *et al.*, 1998; Jacob *et al.*, 2000; Man *et al.*, 2006). Some methods require a large sample volume (1 mL) of plasma (Xu *et al.*, 2004). A liquid chromatography–mass spectrometry (LC-MS) method (McManus *et al.*, 1990; Okano *et al.*, 2007) was reported for the simultaneous detection of NIC and COT in biological fluids. Several liquid chromatography–tandem mass spectrometry (LC-MS/MS) methods have been reported. However, some of the methods require troublesome extraction procedures and/or multiple sample preparation steps prior to the assay. Moreover, these method use a large volume sample (about 0.5–1.0 mL; Bernert *et al.*, 1997; Moyer *et al.*, 2002; Shakleya and Huestis, 2009; Miller *et al.*, 2010). Hydrophilic interaction chromatography–tandem mass spectrometry (HILIC-MS/MS) methods, which measured only NIC and COT, have been reported (Shou and Naidong, 2005; Murphy *et al.*, 2007). Conventional methods have low selectivity and/or require a large volume serum for the determination of analytes. A high-sensitivity and accurate analytical method is needed, using very low volume sample because it is difficult to obtain a large amount of cord blood.

In the present study, we developed a HILIC-MS/MS method for the simultaneous determination of NIC and its metabolites in human serum. This method was used to determine NIC and its metabolites in human maternal and cord sera, to study the effects of the exposure on neonatal outcome.

Experimental

Materials

(–)-Nicotine (NIC) and (–)-cotinine (COT) were purchased from Sigma-Aldrich Japan (Tokyo, Japan). *Trans*-3′-hydroxycotinine (HCOT), (*R,S*)-nornicotine (NNIC) and (*R,S*)-norcotinine (NCOT) were from Toronto Research Chemicals (Toronto, USA). Chemical structures and metabolic pathways are shown in Fig. 1. (±)-Nicotine-d_3 (NIC-d_3), (±)-cotinine-d_3 (COT-d_3), (*R,S*)-nornicotine-d_4 (NNIC-d_4), (*R,S*)-norcotinine-d_4 (NCOT-d_4) and *trans*-3′-hydroxycotinine-d_3 (HCOT-d_3) used as internal standard (IS) were purchased from Toronto Research Chemicals (Toronto, USA). All other reagents of analytical grade were obtained from Wako Pure Chemicals (Tokyo, Japan). Solid-phase extraction (SPE) Oasis MCX (1 mL, 30 mg)

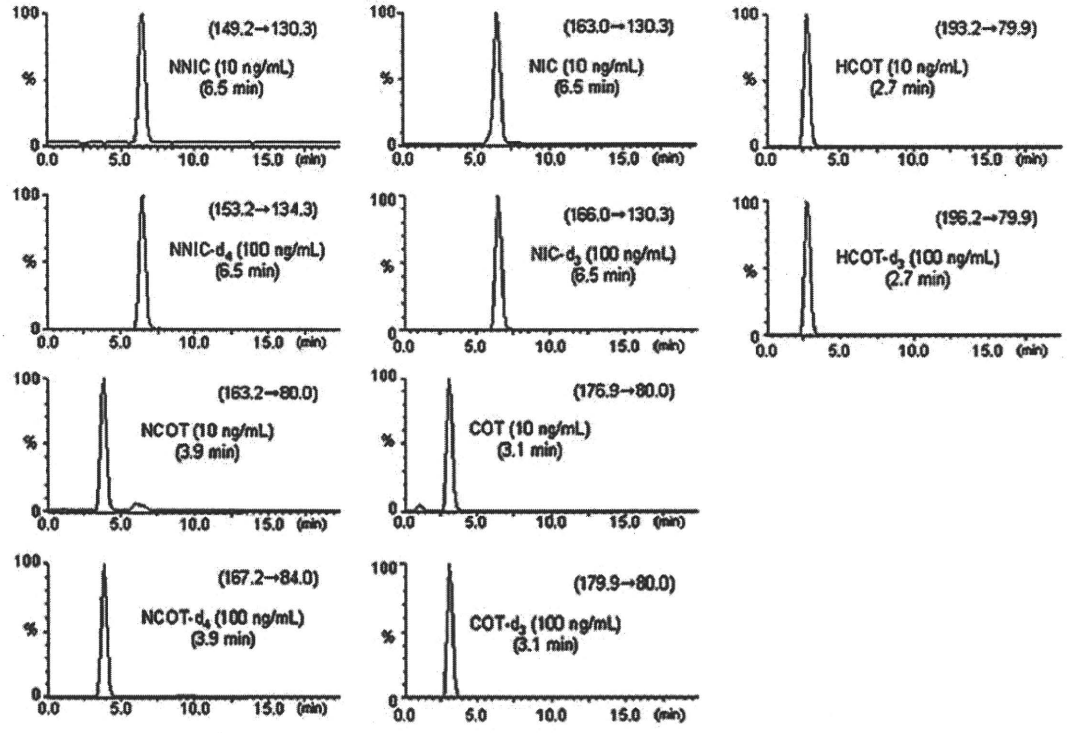

Figure 2. MRM chromatograms of standard samples (10 ng/mL).

Table 2. Recovery test of nicotine and its metabolites in serum samples

Compound	Recovery yield (mean ± SD, %, $n = 6$)				
	LOQ	10 ng/mL	50 ng/mL	100 ng/mL	Matrix effect
NNIC	96.7 ± 5.5	100.3 ± 6.5	103.7 ± 1.0	102.4 ± 2.7	81.7 ± 9.6
NIC	107.6 ± 10.1	90.1 ± 2.6	98.2 ± 2.4	98.6 ± 1.4	75.9 ± 8.5
NCOT	103.3 ± 4.0	107.7 ± 1.9	101.4 ± 8.0	92.2 ± 4.8	97.1 ± 14.8
COT	96.1 ± 6.1	96.6 ± 8.3	97.7 ± 1.4	99.2 ± 1.7	108.9 ± 15.8
HCOT	86.2 ± 11.0	97.3 ± 9.6	101.0 ± 2.7	102.2 ± 2.5	67.4 ± 11.0

cartridges were from Waters (Tokyo, Japan). Deionized water was distilled before passing through a Millipore water purification system.

This study was performed in accordance with the protocol approved by the Institutional Review Board of Yamaguchi University Graduate School of Medicine. Written informed consent was obtained from all study participants. Maternal blood samples were obtained from 20 Japanese normal pregnant women at admission for labor (pregnancy 37–42 weeks of gestation) in Yamaguchi University Hospital. Cord blood samples were obtained immediately after labor. After blood sampling, serum fractions were separated by centrifugation and stored at −80°C until analysis.

LC-MS/MS Conditions

LC-MS/MS analyses were performed using an Alliance HPLC system (Waters, Japan) interfaced to a Micromass Quattro micro API triple quadrupole mass spectrometer (Waters) equipped with an electrospray ionization (ESI) probe. Chromatographic separation was achieved using an Atlantis HILIC column (100 × 2.1 mm, 3.0 µm; Waters, Japan) and a gradient mobile phase. Column temperature was maintained at 40°C and flow rate was set to 0.2 mL/min. Mobile phases were (A) acetonitrile, (B) water and (C) 1% formic acid. A gradient program was used according to the following profile: 0–3 min, 25% B and 5% C; 3–4 min, 25–45% B and 5% C; 4–11 min, 45% B and 5% C; 11–12 min, 45–25% B and 5% C; and 12–20 min, 25% B and 5% C. Autosampler temperature was set to 4°C and 5 µL was injected.

MS/MS characterization of the analytes was achieved using the triple quadrupole with an ESI probe. The analytes that were dissolved in methanol to a concentration of 100 ng/mL were infused through an integrated syringe pump into the ESI probe at a rate of 10 µL/min to tune the mass spectrometer and optimize the acquisition parameters. Optimization results for the two most abundant ion transitions of analytes in the multiple reaction monitoring (MRM) mode are given in Table 1. The following optimized conditions were set: source temperature at 120°C and desolvation temperature at 300°C. Cone and desolvation gas flow rates were set at 50 and 300 L/h, respectively.

Preparation of Standards

Stock solutions of analytical compounds (2 mg/mL) were prepared in methanol. Working solutions of analytical compounds were prepared by serial dilution of the stock solutions in methanol. Quality control (QC) solutions for the determination of accuracy, precision and the stability of samples under storage conditions were added to 100 µL of human serum

Table 3. Validation of LC–MS/MS method for the analysis of nicotine and its metabolites

Compound	Range (ng/mL)	LOD[a] (ng/mL)	LOQ[b] (ng/mL)	*r*	Slope	Intercept
NNIC	7.5–500	0.5	7.5	0.9999	0.0023	−0.0010
NIC	1–500	0.5	1	0.9999	0.0049	0.0008
NCOT	5–500	0.5	5	0.9999	0.0050	−0.0031
COT	1–500	0.5	1	0.9999	0.0019	0.0003
HCOT	1–500	0.5	1	0.9999	0.0053	0.0013

[a] LOD: S/N = 3.
[b] LOQ: S/N > 10, accuracy < 15% and precision <15%.

Table 4. Accuracy, intra-day assay and inter-day assay for serum ($n = 6$)

	LOQ	10 ng/mL	50 ng/mL	100 ng/mL
NNIC				
Accuracy (%)	101.1	92.8	91.2	100.1
Intra-day (%RSD)	3.3	6.5	1.0	2.7
Inter-day (%RSD)	10.8	7.7	9.8	3.1
NIC				
Accuracy (%)	109.2	96.8	101.0	99.4
Intra-day (%RSD)	10.0	2.6	2.4	1.4
Inter-day (%RSD)	7.1	7.4	4.9	2.6
NCOT				
Accuracy (%)	109.0	107.7	105.3	101.6
Intra-day (%RSD)	3.0	1.9	8.0	4.8
Inter-day (%RSD)	8.5	5.4	8.7	7.0
COT				
Accuracy (%)	97.5	98.1	95.4	97.3
Intra-day (%RSD)	7.5	8.3	1.4	1.7
Inter-day (%RSD)	4.8	7.9	4.9	2.5
HCOT				
Accuracy (%)	85.8	95.2	97.2	97.5
Intra-day (%RSD)	10.0	9.6	2.7	2.5
Inter-day (%RSD)	11.1	9.1	2.4	2.1

creating final concentrations from LOQ, 10, 50 and 100 ng/mL, respectively, and stored at −80°C until analysis.

Sample Preparation by Solid-phase Extraction

Serum sample (100 µL) was added to 50 µL of IS solution (200 ng/mL), 750 µL of water and 100 µL of 25% (w/v) trichloroacetic acid to remove proteins. The solutions were centrifuged at 10,000*g* for 5 min after vortexing. The supernatant (900 µL) was applied to SPE cartridges.

An Oasis MCX cartridge (Waters) was conditioned with 1 mL of methanol and 1 mL of water. Serum samples were loaded and allowed to flow by gravity. Cartridges were washed with 1 mL × 2 water and 1 mL methanol, and dried for 5 min. Analytes were eluted with freshly prepared 1 mL × 3 methanol with 1% ammonia (v/v). Eluates were evaporated to dryness under a nitrogen stream at 50°C. Samples were reconstituted in 90 µL of acetonitrile with 0.1% formic acid (v/v) and transferred to polypropylene autosampler vials.

Validation Procedures

Prior to the application to real samples, the method was tested in a validation protocol following the accepted criteria for bioanalytical method validation. Selectivity, recovery, matrix effect, linearity, limits of detection and quantification (LOD and LOQ), precision, accuracy and stability were determined.

Recovery was calculated from the peak area ratios (in percent) of extraction samples to control samples at each concentration. For the evaluation of the matrix effect, the peak areas of extracted pooled serum samples spiked with standards at QC concentrations after the extraction procedure were compared with the peak areas of QC samples.

Calibration curves were tested over the calibration range for all the analytes. Peak area ratios between compounds and IS were used for calculations. The correlation coefficient (r) should be more than 0.99 and deviation of the calculated concentrations should be within ±15% from nominal concentrations.

Five replicates of pooled serum samples were used to calculate LOD and LOQ. The standard deviation (SD) of the mean noise level of each analyte was used to determine LOD (S/N = 3) and LOQ (S/N > 10). To be accepted, the calculated LOQ had to show precision and accuracy within 15% relative SD (RSD) and relative error, respectively.

Six replicates of each of four different QC sample concentrations were analyzed for the determination of intra-day assay precision and accuracy. Inter-day assay precision and accuracy were determined for six independent experimental assays of the aforementioned replicates. Precision was expressed as the RSD of the concentrations calculated for QC samples.

Table 3. Sample stability under several conditions

Sample stability (mean ± SD, %, $n = 6$)	25°C				4°C		−80°C		−80°C[a]	
	1 h	2 h	3 h	6 h	12 h	24 h	24 h	72 h	24 h	72 h
20 ng/mL										
NNIC	100.9 ± 4.2	99.7 ± 5.0	100.4 ± 6.1	100.7 ± 4.2	100.3 ± 7.1	95.4 ± 3.6	99.0 ± 10.2	101.7 ± 7.0	97.5 ± 7.5	109.9 ± 14.6
NIC	91.9 ± 9.1	92.5 ± 10.6	95.9 ± 5.5	102.6 ± 11.9	95.7 ± 6.4	96.9 ± 8.3	98.4 ± 9.4	92.6 ± 12.5	115.1 ± 12.2	101.1 ± 6.0
NCOT	99.7 ± 1.6	101.1 ± 1.2	101.0 ± 1.4	103.6 ± 1.8	98.4 ± 1.2	98.9 ± 1.6	97.5 ± 4.7	109.5 ± 4.5	101.8 ± 1.8	106.1 ± 7.6
COT	98.3 ± 1.2	98.7 ± 2.1	104.8 ± 2.4	102.1 ± 2.4	96.9 ± 2.0	102.2 ± 2.0	109.4 ± 6.0	102.3 ± 6.4	104.8 ± 2.3	100.1 ± 2.4
HCOT	98.6 ± 1.7	98.6 ± 1.5	98.4 ± 1.3	101.0 ± 2.6	97.6 ± 1.3	98.9 ± 1.3	99.9 ± 2.6	95.7 ± 2.1	98.6 ± 1.0	98.0 ± 4.4
100 ng/mL										
NNIC	100.8 ± 2.2	106.7 ± 2.9	103.7 ± 3.7	102.8 ± 2.9	102.8 ± 3.3	106.9 ± 3.2	104.8 ± 3.4	106.6 ± 2.9	109.4 ± 3.5	113.7 ± 9.3
NIC	107.1 ± 10.0	108.9 ± 4.9	105.4 ± 7.4	108.4 ± 12.4	102.5 ± 5.9	104.2 ± 6.5	114.7 ± 17.7	109.8 ± 3.5	111.3 ± 7.0	108.2 ± 5.3
NCOT	104.5 ± 3.5	104.0 ± 1.3	109.2 ± 7.2	102.6 ± 5.0	99.3 ± 3.3	102.0 ± 2.9	102.1 ± 6.8	101.9 ± 3.0	107.2 ± 5.9	99.8 ± 2.3
COT	99.7 ± 1.5	109.3 ± 2.8	110.8 ± 2.0	102.3 ± 2.4	100.3 ± 1.2	109.0 ± 2.0	109.2 ± 4.8	101.7 ± 3.0	112.5 ± 2.6	107.2 ± 5.5
HCOT	102.4 ± 1.8	103.6 ± 1.3	104.2 ± 1.8	103.2 ± 1.3	98.5 ± 1.7	101.5 ± 1.6	102.4 ± 0.9	103.9 ± 3.1	108.3 ± 7.2	106.7 ± 5.7

[a] Freeze–thaw stability of the extract (three cycles).

Accuracy was expressed as the ratio of theoretical concentrations to average measured ones.

Serum sample stability was examined as well: stability of the unprocessed sample (24 and 72 h, −80°C), autosampler stability (6, 12, and 24 h, 4°C), processed sample preparation (1, 2, 3, and 4 h, 25°C), and freeze–thaw stability of the extract (three cycles).

Results and Discussion

Optimization of HILIC-MS/MS Conditions

The analytes that were dissolved in methanol at a concentration of 100 ng/mL were infused through an integrated syringe pump into the ESI probe at a rate of 10 µL/min to tune the mass spectrometer and optimize the acquisition parameters. Comparison of the results obtained in the positive and negative ion modes showed that a high response was obtained in the positive ESI mode. The optimized MRM conditions are given in Table 1.

NIC and its metabolites are highly polar compounds and are thus difficult to determine by reverse-phase liquid chromatography. Several approaches to retaining the desired compound on the stationary phase or separating other compounds are available. HILIC is characterized by the presence of a high initial organic modifier concentration to favor hydrophilic interactions between the solute and the hydrophilic stationary phase (Alpert, 1990). HILIC is an alternative to normal-phase chromatography as it uses a silica column and conventional reverse-phase mobile phase. Thus, the retention times of highly polar compounds are increased as the hydrophilicity of the solute is increased. HILIC can be easily used with a mass spectrometer since it is a variant of normal-phase chromatography. In HILIC, the hydrophilic stationary phase is used in combination with a mostly organic mobile phase, and elution is usually performed by increasing water concentration. HILIC-MS was recently employed to separate and quantify highly polar compounds in biological samples (Iwasaki *et al.*, 2006).

We examined whether the presence of formic acid in the mobile phase would increase both sensitivity and resolution, to obtain sharp peaks. Formic acid improved separation and sensitivity and the mobile phase that gave the most intense peak contained 0.001% formic acid (data not shown). When the mobile phase decreased in concentration and pH value, all compounds increased in peak intensity. However, the lower concentration of formic acid affected the retention time and peak shape of NIC, which was also retained by the HILIC column. For this reason, we concluded that the final concentration of mobile phase was set to 0.05% formic acid. MRM chromatograms are shown in Fig. 2. All analytes were well detected and separated. Moreover, the other compounds did not affect the identification or quantitation even when a high concentration of sample was injected.

Solid-phase Extraction Recovery

Optimization of the SPE procedure was carried out to meet three objectives. First, the overall conditions selected would provide the highest and most consistent absolute recovery of the target analyte. Second, the conditions for washing the SPE cartridges containing bound analyte would remove unwanted matrix components to the greatest extent possible without eluting the target analyte or IS. Third, elution conditions would subsequently recover the analyte efficiently while minimizing the elution of less polar matrix components (Yu *et al.*, 2008). Recovery was calculated from the peak area ratios (in percent) of extraction samples

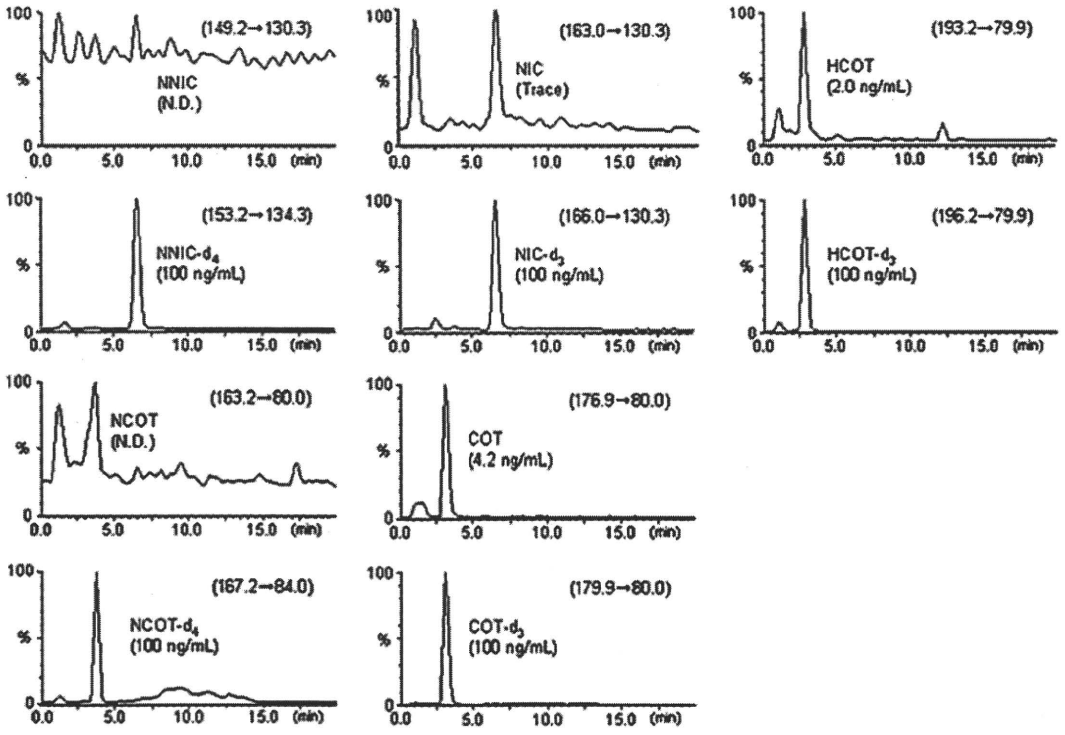

Figure 3. MRM chromatograms of nicotine and its metabolites in maternal serum sample (no. 18).

to control samples at each concentration and the results are shown in Table 2. The recoveries of NIC and its major metabolites, such as COT and HCOT, from human serum samples ranged from 86.2 and 107.7%.

To evaluate the matrix effect, peak areas of extracted pooled serum samples spiked with standards at QC concentrations after the extraction procedure were compared with those of QC samples (Matuszewski *et al.*, 2003; Chambers *et al.*, 2007). Table 2 shows the results of the matrix effect. The results indicated that NIC and its metabolites were influenced by the matrix effect through ion suppression. Although the magnitude of the matrix effect was not determined, the accuracy and precision of the method at this level were found to be within the limits required by the FDA. However, they indicated that matrix effects should be investigated to ensure that precision and sensitivity are not compromised.

Validation

The LODs of the HILIC-MS/MS method were determined by analyzing the response after injecting methanol containing NIC and its metabolites. The LOQs for NIC, COT and HCOT were 1 ng/mL. The correlation coefficient (r) was more than 0.99 and deviation of the calculated concentrations was acceptable within ±15% from nominal concentrations (Table 3). Moreover, in each analytical run, the highest calibrator containing all analytes (500 ng/mL) was injected immediately before a negative sample, allowing the quantification of potential carryover. There was no evidence of carryover at the method's LOD.

Precision and accuracy were assessed at LOQ, 10, 50, and 100 ng/mL. Table 4 contains intra- and inter-day assay precision and accuracy data for each concentration. Precision was determined by multiple analyses of the same sample at different days, and is expressed as RSD. Precision was evaluated by calculating intra- and inter-day assay at each QC concentration. Intra-day assay was less than 10% for all the analytes ($n = 6$). The differences from the target were less than 10% and considered clinically insignificant. Inter-day assay ($n = 6$) was less than 10% for each compound.

Accuracy, also called bias, expresses the similarity of the experimental mean value to the accepted reference value. It indicates systematic errors and is expressed as percentage deviation from the accepted reference value. Accuracy was acceptable in each case (threshold of ±15%) as the relative bias was lower than 14.2%. The RSDs for the intra-day assay as well as for the inter-day assay were within ±15%, which is acceptable according to the FDA guidelines for bioanalytical method validation (FDA, 2001).

The pooled serum sample was spiked with the analyte at 20 or 100 ng/mL and six samples were analyzed immediately following sample preparation. The remaining pooled serum sample was divided into two subsets (stable samples and control samples). Stable samples were stored at 25, 4 and −80°C, respectively (Table 5). Losses of less than 10% were observed on storage for 3 h at 25°C (room temperature storage) and for 24 h at 4°C (autosampler storage). There was no significant degradation and stability was maintained under routine laboratory conditions. Stability studies were conducted to ensure that the analytes were stable during the preparation, processing and analysis.

Application

To demonstrate the applicability of the method, prenatal tobacco-exposed maternal and cord sera were analyzed. One

Table 6. Quantification of maternal and cord serum

Compound	Non-smoker	Smoker			
	Sample No. 1–16	No. 17	No. 18	No. 19	No. 20
Maternal serum					
NNIC	ND	ND	ND	ND	ND
NIC	ND	ND	Trace	3.2	7.8
NCOT	ND	ND	ND	ND	5.4
COT	ND	ND	4.2	13.6	486.4
HCOT	ND	ND	2.0	ND	163.5
Cord serum					
NNIC	ND	ND	ND	ND	ND
NIC	ND	ND	ND	ND	ND
NCOT	ND	ND	ND	ND	2.6
COT	ND	ND	2.5	4.8	216.8
HCOT	ND	ND	1.3	ND	93.9

All values in ng/mL.

maternal serum sample contained 4.2 ng/mL COT and 2.0 ng/mL HCOT. The corresponding chromatograms are displayed in Fig. 3. All nonsmoker maternal and cord serum samples were negative for NIC and its metabolites (Table 6). In smokers, mean cotinine level in maternal serum was 126.1 ± 240.3 ng/mL and mean HCOT level was 41.4 ± 81.4 ng/mL. The concentrations of NIC metabolites in cord serum were generally two- to threefold lower than in serum from the mothers, but strong correlations were observed between maternal and cord serum.

Conclusions

A sensitive and specific HILIC-MS/MS method for the simultaneous detection and quantification of NIC and its metabolites in human maternal and cord sera is presented. The method has sufficient analytical sensitivity for the quantification of analytes using a very low volume of serum (100 µL). The method could be used to determine NIC and its metabolites in human maternal and cord sera in future studies of the effects of nicotine exposure on neonatal outcome.

Acknowledgements

This study was supported by grants from the Ministry of Health, Labour and Welfare, Japan.

References

Abu-Qare AW and Abou-Donia MB. Quantification of nicotine, chlorpyrifos and their metabolites in rat plasma and urine using high-performance liquid chromatography. *Journal of Chromatography B, Biomedical Sciences and Applications*. 2001; **757**: 295–300.

Alpert AJ. Hydrophilic-interaction chromatography for the separation of peptides, nucleic acids and other polar compounds. *Journal of Chromatography* 1990; **499**: 177–196.

Andres RL and Day MC. Perinatal complications associated with maternal tobacco use. *Seminars in Neonatology: SN* 2000; **5**: 231–241.

Benowitz NL. Cotinine as a biomarker of environmental tobacco smoke exposure. *Epidemiologic Reviews* 1996; **18**: 188–204.

Benowitz NL, Jacob P 3rd, Fong I and Gupta S. Nicotine metabolic profile in man: comparison of cigarette smoking and transdermal nicotine. *The Journal of Pharmacology and Experimental Therapeutics* 1994; **268**: 296–303.

Bernert JT Jr, Turner WE, Pirkle JL, Sosnoff CS, Akins JR, Waldrep MK, Ann Q, Covey TR, Whitfield WE, Gunter EW, Miller BB, Patterson DG Jr, Needham LL, Hannon WH and Sampson EJ. Development and validation of sensitive method for determination of serum cotinine in smokers and nonsmokers by liquid chromatography/atmospheric pressure ionization tandem mass spectrometry. *Clinical Chemistry* 1997; **43**: 2281–2291.

Bouckaert A. Smoking during pregnancy: foetal growth retardation and other risks for the newborn. *Statistics in Medicine* 2000; **19**: 239–254.

Bowman TS, Gaziano JM, Buring JE and Sesso HD. A prospective study of cigarette smoking and risk of incident hypertension in women. *Journal of the American College of Cardiology* 2007; **50**: 2085–2092.

Chambers E, Wagrowski-Diehl DM, Lu Z and Mazzeo JR. Systematic and comprehensive strategy for reducing matrix effects in LC/MS/MS analyses. *Journal of Chromatography B, Analytical Technologies in the Biomedical and Life Sciences* 2007; **852**: 22–34.

Davoli E, Stramare L, Fanelli R, Diomede L and Salmona M. Rapid solid-phase extraction method for automated gas chromatographic–mass spectrometric determination of nicotine in plasma. *Journal of Chromatography B, Biomedical Sciences and Applications* 1998; **707**: 312–316.

FDA. *Guidance for Industry. Bioanalytical Method Validation*. US Department of Health and Human Services, Food and Drug Administration, Center for Drug Evaluation and Research, 2001.

Freedman ND, Leitzmann MF, Hollenbeck AR, Schatzkin A and Abnet CC. Cigarette smoking and subsequent risk of lung cancer in men and women: analysis of a prospective cohort study. *The Lancet Oncology* 2008; **9**: 649–656.

Hukkanen J, Jacob III P and Benowitz NL. Metabolism and disposition kinetics of nicotine: *Pharmacological Reviews* 2005; **57**: 79–115.

Iwasaki Y, Hoshi M, Ito R, Saito K and Nakazawa H. Analysis of glutathione and glutathione disulfide in human saliva using hydrophilic interaction chromatography with mass spectrometry. *Journal of Chromatography B, Analytical Technologies in the Biomedical and Life Sciences* 2006; **839**: 74–79.

Jacob P 3rd, Wu S, Yu L and Benowitz NL. Simultaneous determination of mecamylamine, nicotine, and cotinine in plasma by gas chromatography–mass spectrometry. *Journal of Pharmaceutical and Biomedical Analysis* 2000; **23**: 653–661.

Lockman PR, McAfee G, Geldenhuys WJ, Van der Schyf CJ, Abbruscato TJ and Allen DD. Brain uptake kinetics of nicotine and cotinine after chronic nicotine exposure. *The Journal of Pharmacology and Experimental Therapeutics* 2005; **314**: 636–642.

Man CN, Gam LH, Ismail S, Lajis R and Awang R. Simple, rapid and sensitive assay method for simultaneous quantification of urinary nicotine and cotinine using gas chromatography–mass spectrometry. *Journal of Chromatography B, Analytical Technologies in the Biomedical and Life Sciences* 2006; **844**: 322–327.

Matuszewski BK, Constanzer ML and Chavez-Eng CM. Strategies for the assessment of matrix effect in quantitative bioanalytical methods based on HPLC-MS/MS. *Analytical Chemistry* 2003; **75**: 3019–3030.

McManus KT, deBethizy JD, Garteiz DA, Kyerematen GA and Vesell ES. A new quantitative thermospray LC-MS method for nicotine and its metabolites in biological fluids. *Journal of Chromatographic Science* 1990; **28**: 510–516.

Miller EI, Norris HR, Rollins DE, Tiffany ST and Wilkins DG. A novel validated procedure for the determination of nicotine, eight nicotine metabolites and two minor tobacco alkaloids in human plasma or urine by solid-phase extraction coupled with liquid chromatography–electrospray ionization–tandem mass spectrometry. *Journal of Chromatography B, Analytical Technologies in the Biomedical and Life Sciences* 2010; **878**: 725–737.

Moyer TP, Charlson JR, Enger RJ, Dale LC, Ebbert JO, Schroeder DR and Hurt RD. Simultaneous analysis of nicotine, nicotine metabolites, and tobacco alkaloids in serum or urine by tandem mass spectrometry, with clinically relevant metabolic profiles. *Clinical Chemistry* 2002; **48**: 1460–1471.

Murphy SE, Villalta P, Ho SW and von Weymarn LB. Analysis of [3',3'-d(2)]-nicotine and [3',3'-d(2)]-cotinine by capillary liquid chromatography–electrospray tandem mass spectrometry. *Journal of Chromatography B, Analytical Technologies in the Biomedical and Life Sciences* 2007; **857**: 1–8.

Okano K, Hinohara M, Iwasaki Y, Ito R, Saito K, Izumi S-I, Makino T and Nakazawa H. Determination of nicotine and cotinine in human serum for evaluation of tobacco smoke exposure by hydrophilic interaction chromatography/mass spectrometry. *Bunseki Kagaku* 2007; **56**: 785–790.

Pacifici R, Pichini S, Altieri I, Rosa M, Bacosi A, Caronna A and Zuccaro P. Determination of nicotine and two major metabolites in serum by solid-phase extraction and high-performance liquid chromatography, and high-performance liquid chromatography–particle beam mass spectrometry. *Journal of Chromatography* 1993; **612**: 209–213.

Pérez-Stable EJ, Benowitz NL and Marín G. Is serum cotinine a better measure of cigarette smoking than self-report? *Preventive Medicine* 1995; **24**: 171–179.

Pirkle JL, Flegal KM, Bernert JT, Brody DJ, Etzel RA and Maurer KR. Exposure of the US population to environmental tobacco smoke: the Third National Health and Nutrition Examination Survey, 1988 to 1991. *JAMA: the Journal of the American Medical Association* 1996; **275**: 1233–1240.

Pope M, Ashley MJ and Ferrence R. The carcinogenic and toxic effects of tobacco smoke: are women particularly susceptible? *The Journal of Gender-specific Medicine: JGSM: the Official Journal of the Partnership for Women's Health at Columbia* 1999; **2**: 45–51.

Russell MA and Feyerabend C. Cigarette smoking: a dependence on high-nicotine boli. *Drug Metabolism Reviews* 1978; **8**: 29–57.

Seltzer V. Smoking as a risk factor in the health of women. *International Journal of Gynaecology and Obstetrics: the Official Organ of the International Federation of Gynaecology and Obstetrics* 2003; **82**: 393–397.

Shakleya DM and Huestis MA. Simultaneous and sensitive measurement of nicotine, cotinine, *trans*-3'-hydroxycotinine and norcotinine in human plasma by liquid chromatography–tandem mass spectrometry. *Journal of Chromatography B, Analytical Technologies in the Biomedical and Life Sciences* 2009; **877**: 3537–3542.

Shou WZ and Naidong W. Simple means to alleviate sensitivity loss by trifluoroacetic acid (TFA) mobile phases in the hydrophilic interaction chromatography–electrospray tandem mass spectrometric (HILIC-ESI/MS/MS) bioanalysis of basic compounds. *Journal of Chromatography B, Analytical Technologies in the Biomedical and Life Sciences* 2005; **825**: 186–192.

Windham GC, Hopkins B, Fenster L and Swan SH. Prenatal active or passive tobacco smoke exposure and the risk of preterm delivery or low birth weight. *Epidemiology (Cambridge, Mass.)* 2000; **11**: 427–433.

Xu X, Iba MM and Weisel CP. Simultaneous and sensitive measurement of anabasine, nicotine, and nicotine metabolites in human urine by liquid chromatography–tandem mass spectrometry. *Clinical Chemistry* 2004; **50**: 2323–2330.

Yu H, Straubinger RM, Cao J, Wang H and Qu J. Ultra-sensitive quantification of paclitaxel using selective solid-phase extraction in conjunction with reversed-phase capillary liquid chromatography/tandem mass spectrometry. *Journal of Chromatography A* 2008; **1210**: 160–167.

Journal of Reproduction and Development, Vol. 56, No. 1, 2010

—Full Paper—

Resistance to 5-aza-2′-deoxycytidine in Genic Regions Compared to Non-genic Repetitive Sequences

Hui Wen LIM[1)], Misa IWATANI[1)], Naoko HATTORI[1)], Satoshi TANAKA[1)], Shintaro YAGI[1)] and Kunio SHIOTA[1)]

[1)]*Laboratory of Cellular Biochemistry, Animal Resource Sciences/Veterinary Medical Sciences, The University of Tokyo, Tokyo 113-8657, Japan*

Abstract. The DNA methyltransferase (Dnmt) inhibitor and demethylating agent 5-aza-2′-deoxycytidine (5azadC) has been used to induce cellular differentiation and gene activation. It has been approved for treating several kinds of malignancies due to its ability to reactivate silenced tumor suppressor genes. Considering the potential effect of 5azadC on non-targeted genomic regions in normal cells, we investigated its effect on repetitive sequences and selected gene loci, *Oct-4*, *Sall3*, *Per1*, *Clu*, *Dpep1* and *Igf2r*, including tissue-dependent and differentially methylated regions, by treating mouse NIH/3T3 fibroblast cells with concentrations of 5azadC ranging from 0.001 to 5 μM. Demethylation of minor satellite repeats and endogenous viruses was concentration dependent, and the demethylation was strong at 1 and 5 μM. In genic regions, the methylation level decreased only at 0.1 μM, but was minimally altered at concentrations lower or higher, regardless of the abundance of CpG sites. Thus, repeats are strongly demethylated, but genic regions are only demethylated at effective doses. Genes were activated by 5azadC treatment and were accompanied by a unique combination of histone modifications in genic regions, including an increased level of H3K9me3 and a decreased level of AcH3. Increase of H3K9me3 in genic regions was not observed in Dnmt knock out cells. We identified differential effects of 5azadC on repetitive sequences and genic regions and revealed the importance of choosing appropriate 5azadC doses to achieve targeted gene recovery.

Key words: 5-aza-2′-deoxycytidine, Decitabine, DNA methylation, Epigenetics, Histone modification

(J. Reprod. Dev. 56: 86–93, 2010)

DNA methylation is one of the epigenetic events associated with gene regulation and function. Hypermethylation of promoter regions of tumor suppressor genes causes silencing of the genes that lead to cancer [1–3]. Thus, reversing the methylation status of gene promoters to their prevalent methylation states has become a treatment option for certain cancer types. To date, there are many types of demethylating agents that have been shown to inhibit promoter methylation and reactivate silenced genes [4–6]. Some of these have been approved or are in clinical studies to be developed as cancer drugs [7].

The cytosine analog 5-aza-2′-deoxycytidine (5azadC), also known as decitabine, has been widely used as a DNA methyltransferase (Dnmt) inhibitor to reverse aberrant hypermethylation [8, 9]. It has been approved for hematological malignancies, showing favorable results with low dose treatment [10, 11]. Known to have dual modes of action, 5azadC at low doses induces gene hypomethylation, whereas high doses of 5azadC induce cytotoxicity and cause severe side effects in patients [12, 13].

Nearly 40% of the mouse genome is composed of repetitive sequences including different classes of interspersed repeats, such as LINEs, SINEs, LTR elements and satellites, that are mainly found in heterochromatin regions [14]. Most repeats are densely methylated, and methylation in repeats reflects the global methylation level [15, 16]. Loss of methylation in repeats causes genomic instability [17, 18]. Conversely, genes comprise only a small portion of the genome. Tissue-dependent and differentially methylated regions (T-DMRs) are unique sequences in genic regions that are methylated depending on tissue or cell types. T-DMRs have been widely observed, including in undifferentiated embryonic stem cells, normal tissues and even in cloned mice [19–21]. Both repetitive regions and T-DMRs serve as important markers for methylation analysis, as repeats could be used to estimate global methylation, whereas T-DMRs could serve as references for cell- or tissue-specific methylation.

Previous reports show that Dnmts exhibit functional cooperation on genomic regions [22, 23]. We reported previously that Dnmt1, Dnmt3a and Dnmt3b share targets in the same CpG islands with T-DMRs, and each Dnmt has target preferences depending on the genomic regions [24]. Dnmt3a and Dnmt3b prefer T-DMRs of genic regions, whereas Dnmt1 prefers repetitive sequences.

The demethylating effect of 5azadC is exerted by binding to Dnmts [4]. Since Dnmts have multiple targets, there is the potential of having a genome-wide demethylating effect when using 5azadC. Demethylation of non-targeted genomic regions might occur, not only in cancer cells but also in normal cells. In addition, there are diverse interactions between DNA methylation and histone modifications in euchromatic and heterochromatic regions [25, 26]. The epigenetic status of T-DMRs is regulated by the interplay between DNA methyltransferases, histone modification enzymes, nuclear proteins and other epigenetic factors that cooperate to form cell- and tissue-specific DNA methylation profiles [27,

Received: March 17, 2009
Accepted: October 3, 2009
Published online in J-STAGE: December 9, 2009

Correspondence: K Shiota (e-mail: ashiota@mail.ecc.u-tokyo.ac.jp)

28]. It may be possible to induce hypomethylation-independent activation of gene expression and downstream responses. To know whether 5azadC induces an invariable effect on different genomic regions, we investigated the effect of 5azadC on non-genic repetitive sequences and some genic regions including T-DMRs in fibroblast cells.

Materials and Methods

Reagents, cell culture and genome extraction

All reagents were purchased from Wako Pure Chemicals (Osaka, Japan) unless stated otherwise.

NIH/3T3 cells were cultured in Dulbecco's modified Eagle's medium (DMEM; Invitrogen, Carlsbad, CA, USA) supplemented with 10% fetal bovine serum (JRH, Lenexa, KS, USA) and 50 unit/ml penicillin / 50 μg/ml streptomycin (Invitrogen) at 37 C in 5% CO_2 in air. Prior to treatment with 5-aza-2'-deoxycytidine (5azadC; Sigma-Aldrich, St. Louis, MO, USA; diluted with sterile water to the concentrations required), cells were plated at 1×10^5 cells/150 mm dish and cultured for 24 h. Cells were treated with 5azadC to final concentrations ranging from 0.001 to 5μM. Sterile water was substituted for 5azadC in the untreated control. The medium was changed every 24 h, and cells were collected after 3 days for DNA extraction.

Wild type ES cells (J1) and mutant ES cells deficient in *Dnmt*1 (*Dnmt*1$^{-/-}$; c/c), *Dnmt*3a and *Dnmt*3b (*Dnmt*3a$^{-/-}$3b$^{-/-}$; 7aabb) were cultured on gelatin coated dishes with ES medium containing 1000 U/ml leukemia inhibitory factor (Chemicon, Temecula, CA, USA) as previously described [24]. J1, c/c and 7aabb cells were harvested at passage numbers 32, 17 and 17, respectively.

Cells were incubated in lysis buffer (150 mM EDTA, 10 mM Tris-HCl, pH 8.0, and 1% SDS) containing 10 mg/ml proteinase K (Merck, Darmstadt, Germany) at 55 C for 20 min. Following phenol/chloroform/isoamyl alcohol extraction twice, genomic DNA was precipitated with ethanol and dissolved in TE buffer (10 mM Tris-HCl, 1 mM EDTA, pH 8.0).

Cell proliferation assay

NIH/3T3 cells were seeded into 96-well plates at 1×10^3 cells per well, 24 h before 5azadC was added. Cells were treated with 5azadC at final concentrations of 0 (as the control), 0.001, 0.005, 0.01, 0.05, 0.1, 0.5, 1.0, 5.0 and 10.0 μM for 3 or 4 days at 37 C in 0.5% CO_2 in air with medium changes every 24 h. Four hours before plate reading, 10 μl of Cell Proliferation Reagent WST-1 (Roche, Penzberg, Germany) was added. The absorbance of each sample was measured against a background control using an ELISA reader at an absorption wavelength of 450 nm.

Analysis of the methylation status of repetitive sequences by Southern blotting

Genomic DNA (5 μg) was digested with the restriction enzyme *Msp*I (Takara, Kyoto, Japan) or *Hap*II (Takara) and electrophoresed on a 0.8% agarose gel. Following hydrolyzation with 0.25 N HCl and denaturation with 1.5 M NaCl/0.5 N NaOH, the DNA was transferred onto a nylon membrane. The membrane was probed with pMO for endogenous C-type retrovirus (MoMuLV; Genbank accession NC_001501) and pMR150 for minor satellite repeats (X14469 and X07949). Probes were labeled with the Gene Images random prime labeling module (Amersham Pharmacia, Little Chalfont, Buckinghamshire, UK). Hybridization and detection were performed using the Gene Images CDP-star detection module (Amersham Pharmacia) according to the manufacturer's instructions.

Bisulfite restriction mapping and sequencing

Genomic DNA, digested with *Eco*RI, was denatured by incubating with 0.3 M NaOH at 37 C for 15 min. Sodium metabisulfite (pH 5.0) and hydroquinone were added to a final concentration of 2 M and 0.5 mM, respectively, and the mixture was incubated at 55 C for 18 h in the dark. Bisulfite modified DNA was purified with the Wizard DNA Clean-Up System (Promega, Madison, WI, US), and the bisulfite reaction was terminated with NaOH at a final concentration of 0.3 M at 37 C for 15 min. The sample was neutralized by adding NH_4OAc, pH 7.0 (3 M, final concentration), and was precipitated with ethanol. Purified DNA was dissolved in sterile water and amplified using Immolase (Bioline, Tokyo, Japan) with the primer sets as follows: 5'-TAAGGGTAGGTATATAGGTGTGGT-3', F, and 5'-TCTACCCCCTTTAAAAATCACTTTAA-3', R, for ODE; 5'-TGGGTTGAAATATTGGGTTTATTT-3', F, and 5'-CTAAAACCAAATATCCAACCATA-3', R, for OPR; 5'-GGGAAGGGGATTTTGTTATTGTAGT-3', F, and 5'-CATAAACCCAACAACAAACCCATCT-3', R, for *Per1*; 5'-GTTAGGGTTTTTTTAG-GGTATTAGT-3', F, and 5'-CCCTAATCTACCCAACATATACAAA-3', R, for *Sall3*. The PCR conditions were as follows: 95 C for 10 min, followed by 40 cycles of denaturation at 94 C for 30 sec, annealing at 55 C for 30 sec and extension at 72 C for 1 min, with a final extension at 72 C for 10 min.

Oct-4 distal enhancer, *Oct-4* proximal enhancer and promoter PCR products were digested with *Taq*I (Takara) at 65 C, and *Per*1 and *Sall*3 PCR products were digested with *Hpy*CH4IV (NEB, Ipswich, MA, USA) at 37 C for 3 h. Restricted fragments were assessed by agarose gel electrophoresis. Images were recorded and semi-quantified using the ImageJ software provided by the National Institutes of Health (http://rsbweb.nih.gov/ij/). The relative DNA methylation level of each genic region was calculated by the formula: DNA methylation status (%)=$100 \times I^C / (I^{UC} + I^C)$, where I^C and I^{UC} represent the intensities of the digested and undigested bands, respectively.

For bisulfite sequencing, PCR products were cloned into pGEM T-Easy vector (Promega, Madison, WI, USA), and 10 clones were sequenced for each sample. The primer sets used were 5'-TGGGCTGAAATACTGGGTTCACCC-3', F, and 5'-CTGAAGCCAGGTGTCCAGCCATG-3', R, for *Oct-4*; 5'- GGTTGGGGAATTGGTTGTT-3', F, and 5'-CAACCTACTCCTAAATCCTCCA-3', R, for *Dpep1*; 5'- TAGTGAGTGGGGATGTAGTATTATGG-3', F, and 5'-AACCCCTAAACAACTTCAAAATTTT-3', R, for *Clu*; and 5'-GTTTAGAATATTGGTGAGTAGTGGG-3', F, and 5'-CCTTAAAATAAAAATAAACATCTTAAA-3', R, for *Igf2r*, with the following PCR conditions: 95 C for 10 min, followed by 40 cycles of denaturation at 94 C for 30 sec, annealing at 55 C for 30 sec and extension at 72 C for 1 min, with a final extension at 72 C for 10 min.